

Building complex velocity models using equivalent offset migration (EOM) - a case study

M. Graziella Kirtland Grech and John C. Bancroft

ABSTRACT

Equivalent Offset Migration has been used to produce a prestack time migrated section from numerical model data, that provides a better overall image than Kirchhoff prestack time migration using the known velocity model. Better focussing of events and more structural detail make the complex geometry easier to interpret. This improved time migrated section will provide a better starting point for depth migration velocity model building.

INTRODUCTION

It areas where strong lateral velocity variations exists, as in fold-thrust belts, areas of complex overburden or where significant lateral changes in lithology are present, depth migration is required to obtain a good image (Yilmaz, 1987). However, this requires an accurate velocity model of the subsurface, which at times can be very difficult to obtain. Building a velocity model for depth migration is an iterative process and requires any velocity information that is available. This could be from well logs and/or from seismic data by doing primary and residual moveout analysis on unmigrated and image gathers (Shultz and Canales, 1997).

Velocity model building for depth migration usually starts from picking the key horizons on a time migrated section, so the better the image of the time migrated section, the better the initial velocity model. In this study, we have used Equivalent Offset Migration (EOM) to obtain a prestack time migrated section of a complex geological model (Kirtland Grech et al., 1998), assuming no initial knowledge of velocities in the area. The final image is better than that obtained with Kirchhoff prestack migration with the known velocity model, making interpretation easier. This can help build a better initial model for depth migration.

EQUIVALENT OFFSET MIGRATION

Equivalent Offset Migration (EOM) is a prestack time migration based on the Kirchhoff time migration method, which provides better velocity information than conventional methods. It is divided into two steps:

- (a) Formation of Common Scatter Point (CSP) gathers - a gathering process that sums the input traces into *equivalent offset* bins within each CSP gather.
- (b) Separate Kirchhoff migration of each CSP gather - an imaging process.

Formation of CSP gathers

The *equivalent offset* is defined by converting the Double Square Root (DSR) equation, which is derived from the raypaths in Figure 1, into a hyperbolic form, containing only one square root. The latter is achieved by defining a new source and receiver, which are collocated at the equivalent offset position E as shown in Figure 2. The equivalent offset has the same total travel time $2t_e$ as the original path t . The equivalent offset, h_e , is obtained by equating the travel time for the equivalent offset raypath with the DSR to get:

$$h_e^2 = x^2 + h^2 - \left(\frac{2xh}{tv_{mig}} \right)^2$$

where: x is the distance from common mid-point to common scatter point, h the half source-receiver offset and v_{mig} is the migration velocity, which is the RMS approximation of Tanner and Koehler (1978).

When the energy of a particular scatter point is considered as a function of the equivalent offset, it will be distributed along a hyperbolic path that is illustrated in Figure 2. If all traces are ordered according to their equivalent offset from a presumed scatter point, new prestack migration gathers - Common Scatter Point (CSP) gathers - can be formed. No time shifting is used when the energy is copied from each input trace (within the migration aperture) to all CSP gathers. In practice, the equivalent offset is divided into discrete bins and all the energy within a particular bin is summed.

Kirchhoff NMO and stacking of the CSP gathers

Once the CSP gathers are formed, the following steps are applied: scaling, filtering, NMO correction and stacking. These complete the prestack migration process and are equivalent to a Kirchhoff migration of the CSP gather (Bancroft et al., 1998).

Advantages of Velocity Analysis on CSP gathers

- 1) CSP gathers may be formed initially at a few locations with an estimated velocity, and then the resulting gathers can be used to define more accurate velocities. The iterations of this process converge very rapidly.
- 2) CSP gathers show improved velocity resolution on semblance plots when compared to those obtained from a super CMP gather (formed by summing adjacent CMP gathers). This is due to the increased offset range and high fold of CSP gathers. In addition, the velocity information of dipping events is conserved, as the CSP gather is formed at one location as opposed to the spread of a super CMP gather (Bancroft et al., 1998).

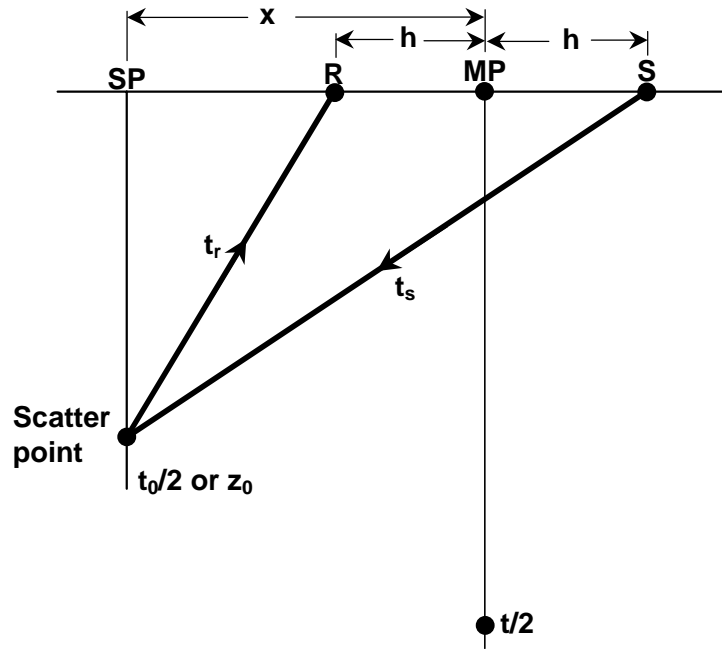


Fig. 1. Raypath from source S to scatter point to receiver R . MP is the mid-point, h is the half-offset and x is the distance between the scatter point and the midpoint. The diagram shows the geometry for Kirchhoff prestack time migration (from Bancroft et al., 1998).

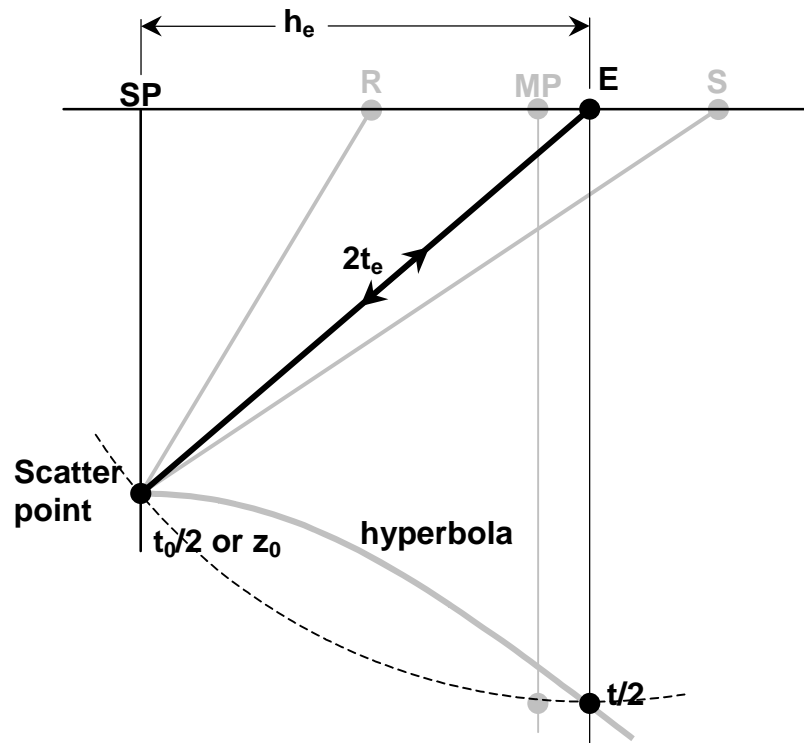


Fig. 2. Raypath for collocated source and receiver at E with the equivalent offset h_e (from Bancroft et al., 1998).

NUMERICAL MODELLING

The geological model

The geological model used for the experiments (Figure 3) was created by Dr. D. A. Spratt and is based on a cross-section through the Foothills and Front Ranges of the Rocky Mountains (Kirtland Grech et al., 1998). The four major areas of interest from the imaging point of view are marked A, B, C and D. These are the Heart Mt. Structure, Mt. Yamnuska, the Panther Culmination and a footwall syncline respectively.

Data Generation

Ray-tracing was done in GX2, using a split-spread type geometry, with a receiver spacing of 50 m and a shot spacing of 200 m. Spread length was 6000 m on either side and the nearest offset was 50 m. After ray tracing, synthetic seismic traces were generated. The generated traces were 6000 ms long, with a sampling interval of 2 ms. The traces were convolved with a Ricker wavelet (peak frequency = 30 Hz) and were then exported as a seg-y file into ProMAX for processing and migration.

PROCESSING

Creation of CSP gathers and EOM

After building the geometry in the usual way, the first step for EOM is the creation of CSP gathers. The velocity function required to create the first set of gathers was obtained by doing velocity analysis at 3 arbitrary locations on CDP gathers. Once the first set of CSP gathers were created, velocity analysis was then done again every 3 km to generate another set of CSP gathers. The same velocity function was smoothed and used for the final part of EOM to provide a migrated image. Velocity analysis was then done again every 500 m or 100 m as required to generate the 3rd set of CSP gathers that was used to create the final migrated image of Figure 10b. With every iteration, the semblance plots became more focussed, making velocity picking easier. In this way the velocity model was improved with each iteration.

Experiments with EOM

The following section describes in detail the various experiments done using the above-mentioned procedure to determine the best parameters for EOM and obtain a good migrated image.

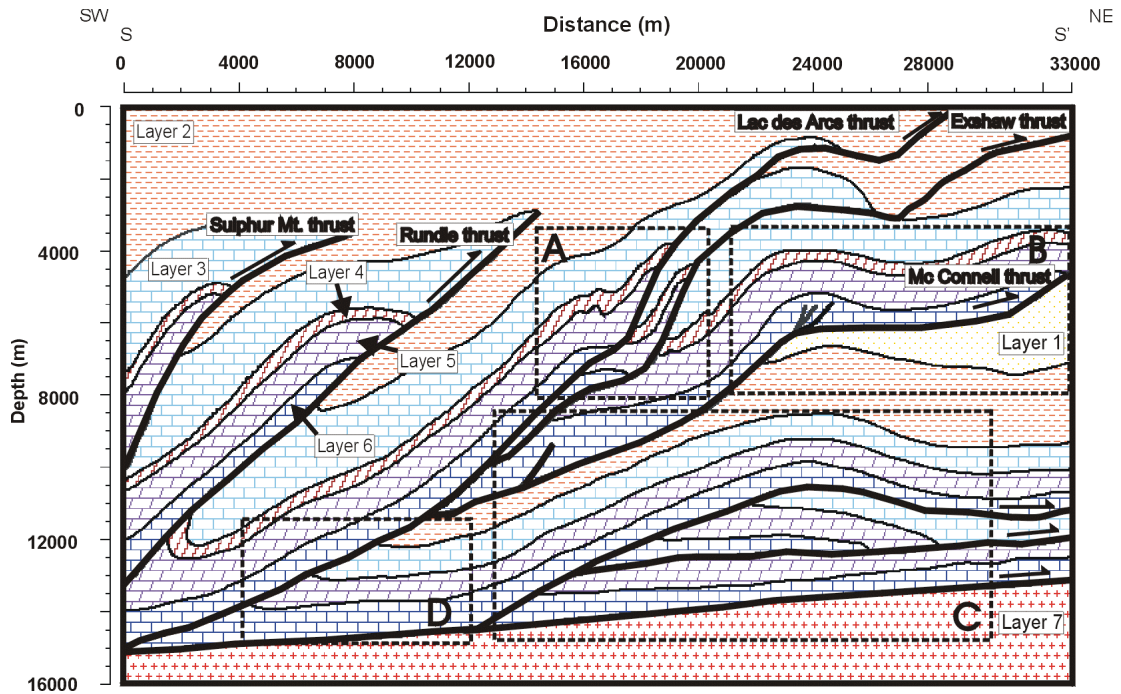


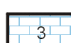






Fig. 3. The geological model - lithology and velocities of each layer are given in Table 1. A - Heart Mt. Structure; B - Mt. Yamnuska; C - Panther Culmination; D - Footwall Syncline.

Table 1. Velocities and lithology description for the different layers shown in Fig. 3.

Layer Number	Period dominant lithology	Velocity (m/s)
	Upper Cretaceous (sandstone + shale)	3900
	Jurassic / Lower Cretaceous shale, sandstone + coal	4250
	Triassic, Permian, Pennsylvanian, Mississippian (Rundle) limestone	6100
	Mississippian (Banff) shale	5500
	Devonian dolomite + limestone	6400
	Cambrian limestone	6250
	Basement igneous / metamorphic	6500

Offset length for forming CSP gathers

Figures 4 and 5 show the same CSP gather formed with an offset of 5000 m (Figure 4a) and 15000 m (Figure 5a). The corresponding semblance plots are shown in Figures 4b and 5b. Figure 5a shows that there is still energy on the CSP gather at offsets greater than 5000 m, particularly between 3000 ms and 5000 ms. This energy can be used to produce better focussing of the deeper events on the semblance plots. Comparison of Figures 4b and 5b, shows how the longer offset range used to create the semblance plot shown in Figure 5b, produces much better focussing of the deeper events than those in Figure 4b. This would make velocity picking on longer offset CSPs much easier. These large offsets are not typical of CDP gathers, hence resolution on CDP gathers will be poorer. The main drawback of using longer offsets to form the CSP gathers is increased computation time and a larger data volume.

Adding random noise to the synthetic dataset

The original synthetic dataset used to form the CSP gathers was noise free. However, it was noticed that in the formation of semblance plots, there were false semblance values that interfered with the semblance peaks associated with the true events. This was attributed to the fact that in the formation of the semblance plots, energy was being picked up from the edge of events on the CSP gathers, and forming artificial semblance values that are swept across the semblance plot as indicated by the arrows in Figure 6a. Addition of some random noise to the synthetic dataset (-20dB) eliminated this undesirable effect and also resulted in more focussed semblance peaks (Figure 6b). As real datasets do contain signal and noise, this issue should not present any problems.

Complex geology and its effect on CSP gathers and semblance plots

Figures 7a and 7b show a CSP gather and its corresponding semblance plot respectively. This CSP is taken from the NE part of the model, on the left slope of the Panther Culmination (C). The low velocity wedge above the Panther Culmination is causing the "hyperbolae" on the CSP gathers to be tilted and with a vertex off the centre. Furthermore, the hyperbolae are "divided": the flat part giving rise to a peak on the semblance plot at a low velocity, while the sloping part gives a peak at higher velocity at a different time. This effect can be seen on the semblance plot in Figure 7b, particularly below 3000 ms, where the peaks seem to be aligned in two columns at about 3000 m/s and 5500 m/s. The isolated peaks at the lower velocity are easier to pick and do result in better imaging of the duplex. However, this trend in semblance peaks changes as the duplex is traversed. The semblance peaks tend to higher velocities over the peak and then again to this split trend over the right hand flank of the structure. Picking the low velocities over the sides and the high velocities over the crest of the structure, lead to abrupt changes in the velocity model, and hence discontinuities in the image (Figure 9b). When the high velocities were picked across the whole structure, the events were over-migrated and resulted in a collection of "smiles" (an over-migration effect similar to that seen on Figure 9a, with Kirchhoff time migration). This problem cannot be solved with time migration and depth migration using an accurate velocity model is needed. However, we are examining what aspects of time migration can be applied to produce the best possible image.

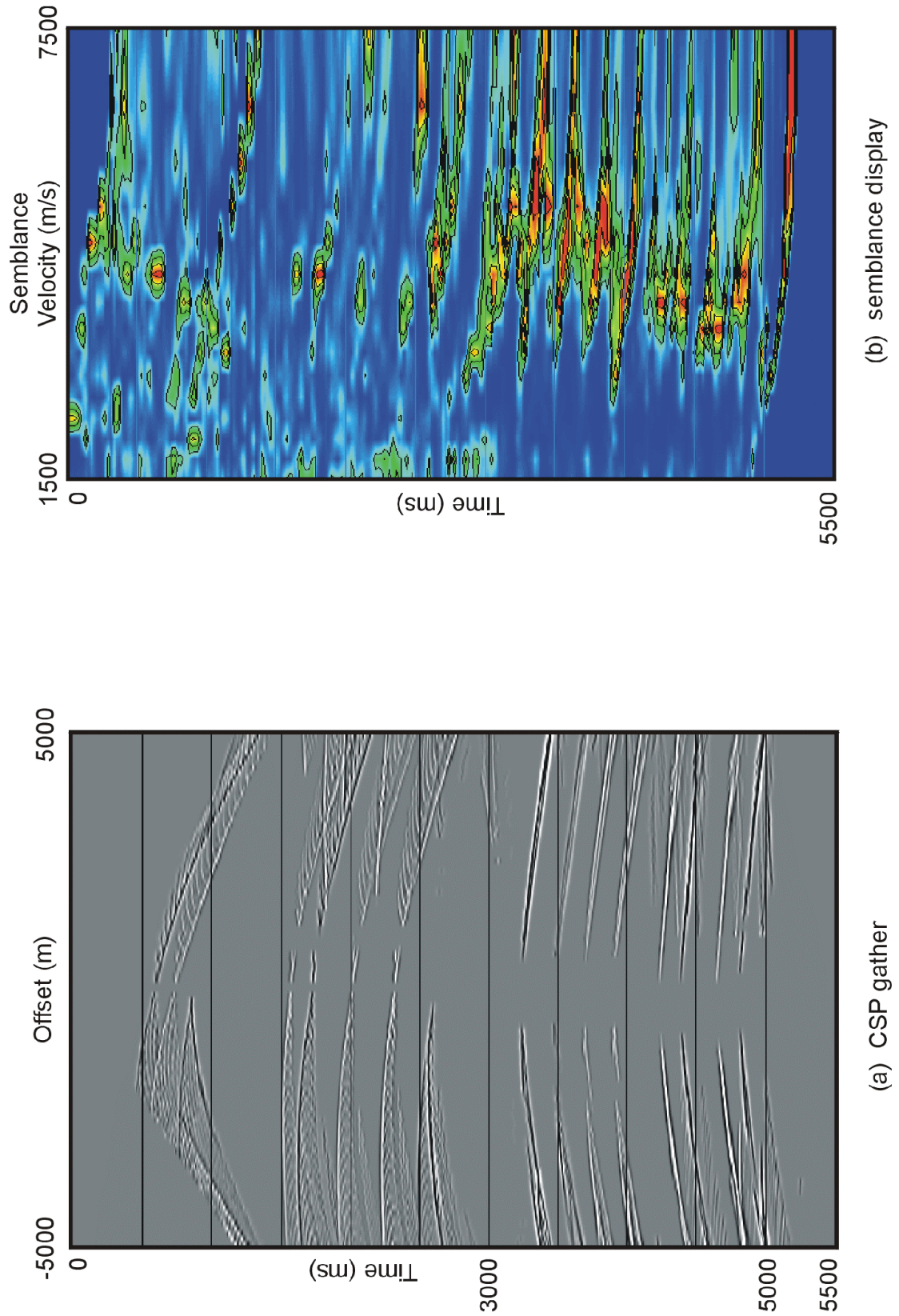


Fig. 4. A double-sided CSP gather formed with an offset of 5000 m (a) and the corresponding semblance display (b).

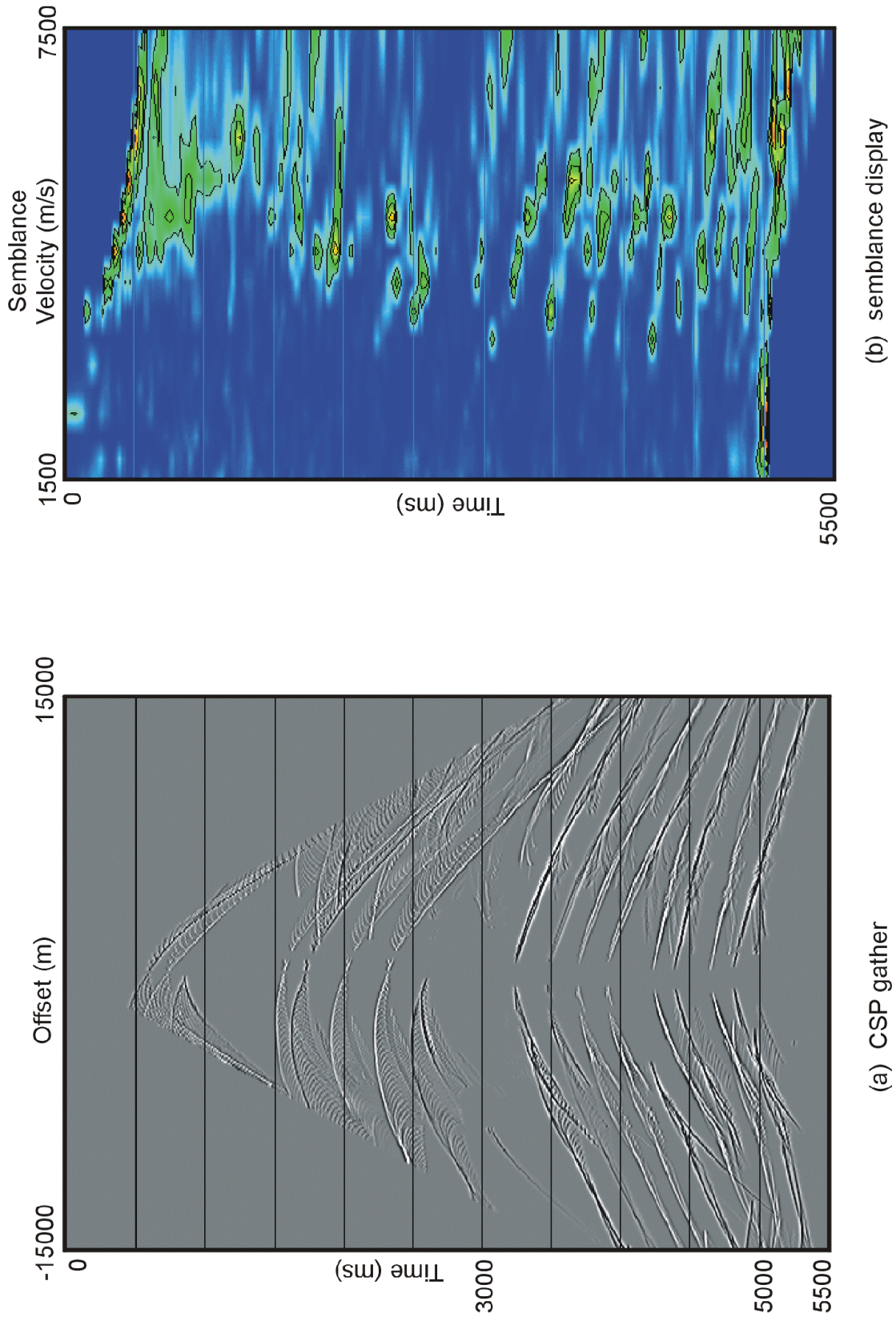


Fig. 5. A double-sided CSP gather formed with an offset of 15000 m (a) and the corresponding semblance plot (b). Note the better focussing due to the increased offsets.

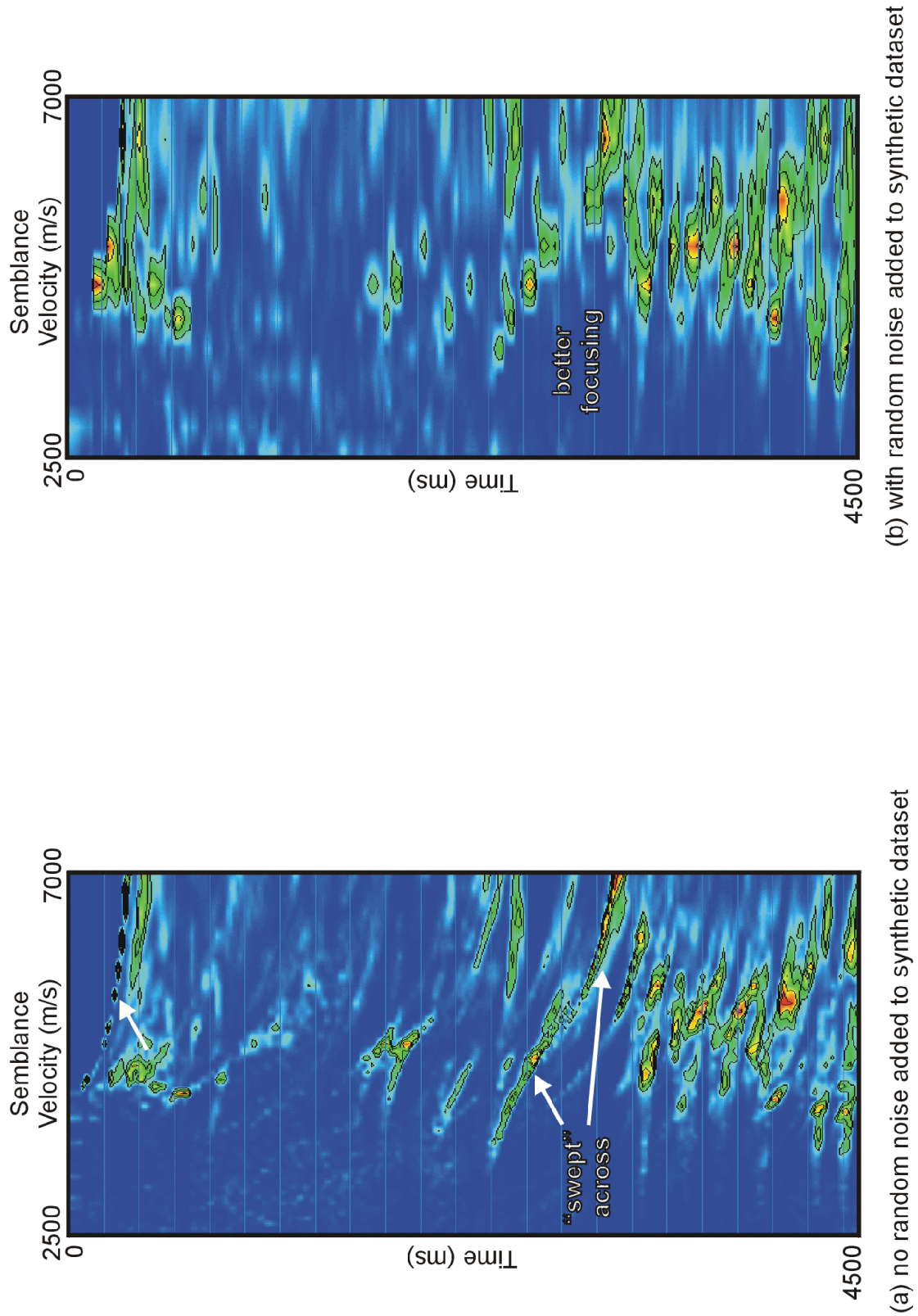


Fig. 6. Comparison of semblance plots. Velocity picking is easier on (b) where there is better focussing and events are not "swept" across the plot as in (a).

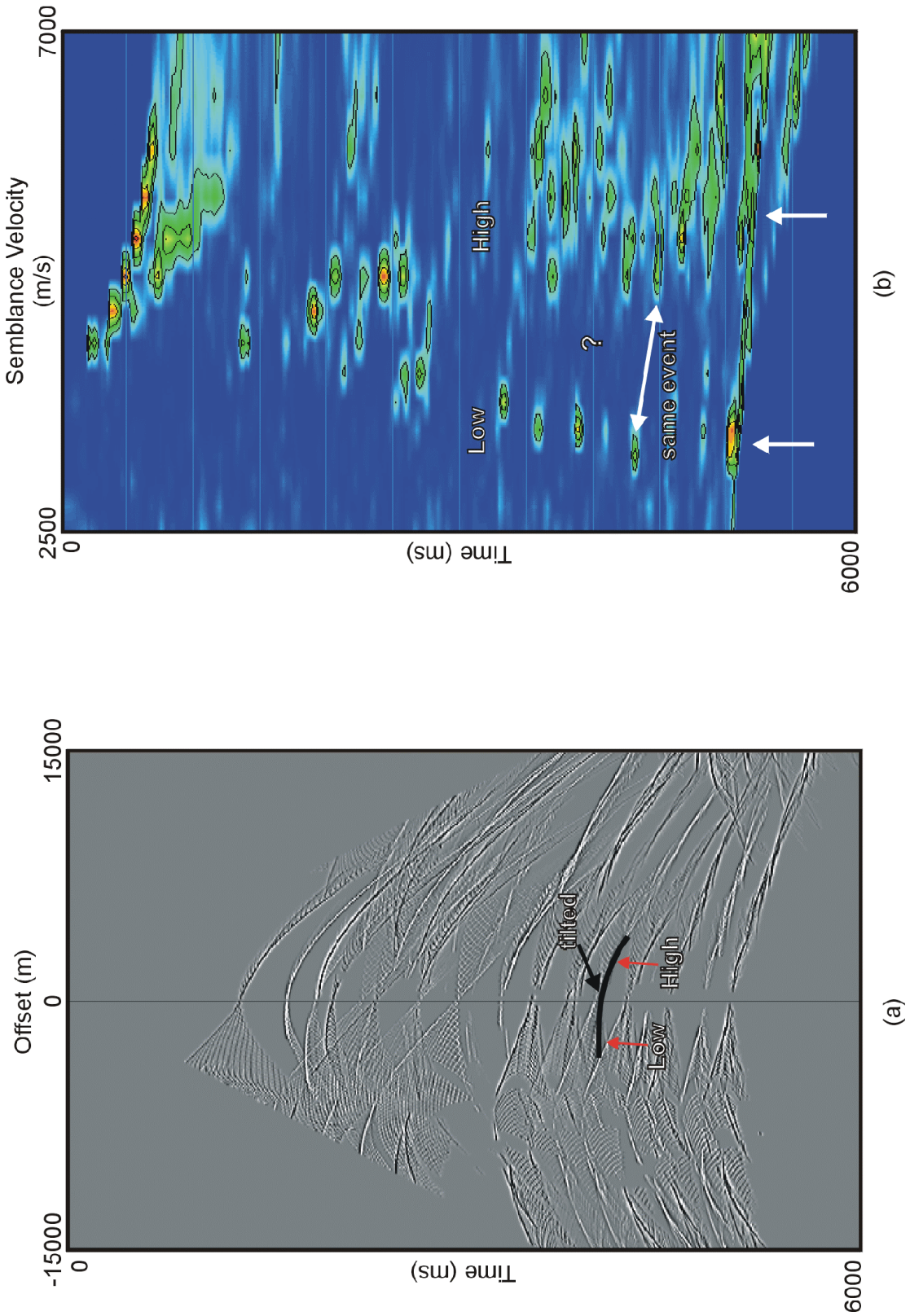


Fig. 7. (a) CSP gather showing tilted, off-centred hyperbolae with "flat" and "sloping" parts, (b) corresponding semblance plot with peaks aligned at low and high velocities.

One-sided versus two-sided CSP gathers

CSP gathers can be formed using both positive and negative offsets, hence forming two-sided CSP gathers, or positive offsets only, resulting in one-sided CSP gathers. Figures 8a and 8b show a two-sided and one-sided CSP gather respectively. The two-sided CSP gather contains more information, making identification of events and velocity picking easier. It also helped understand the tilted hyperbolae previously described.

Frequency of Velocity Analysis locations on the final image

As mentioned earlier, the first velocity field used to generate the CSPs was based on only three analysis locations. Then velocity analysis was done every 3 km on these newly formed CSPs, the resulting velocity field was smoothed and a new set of CSP gathers was formed. Velocity analysis was finally done every 500 m, increasing the interval to 100 m towards the middle of the section, where steep limbs and small scale features are present. Figure 9a and 9b show the final image obtained by doing velocity analysis every 3 km and every 500 m respectively. The dotted area in Figure 8b, encloses the major improvements achieved by having closer velocity analysis. Events carried in the hanging wall of the Lac des Arcs, Exshaw and Mc Connell thrust that are either not imaged at all or very poorly imaged in Figure 9a, can now be interpreted. Also, the different layers of the Panther Culmination (C) are better focussed as opposed to the same events in Figure 9a. This was achieved by biasing the semblance picks towards the low velocities, as discussed above. Closer velocity analysis locations also resulted in better imaging of the small scale features of the Heart Mt. Structure (A).

Effects of smoothing the velocity model used for stacking

Using the actual picks for the velocity model leaves the events looking rough, giving an impression of false structure (Figure 10a). Smoothing the velocity field (Figure 10b) greatly enhances the overall image, although where velocity changes were large, the smoothing did not work very well (indicated by arrows on Figure 10b). This is attributed to the fact that smoothing is done horizontally, instead of along gradients for dipping events. This problem can be overcome by doing velocity analysis at more closely spaced locations, so that the gradient of the dipping events can be approximated when smoothing is done. However, this would be extremely time consuming. Since interpretation of Figure 9b can be done with a certain degree of confidence, this problem was not tackled further. The number of analysis points could be reduced with an interpolator that followed the dips of the events.

Comparison of EOM with prestack Kirchhoff time migration

Figure 11a shows a Kirchhoff prestack time migrated section with the velocities derived from the actual model. This velocity model was obtained by a conversion (using vertical rays) from interval velocities in depth to RMS velocities, which are required by the Kirchhoff prestack time migration module. Conversion along image rays would yield a better velocity model. The Kirchhoff prestack migration (Figure 11a) is to be compared with Figure 11b which shows the EOM result, where the velocity model was built from scratch. Interpretation of the EOM section (Figure 11b)

is certainly easier than interpreting the Kirchhoff migrated section (Figure 11a), especially in the enclosed section. The Panther Culmination (C), although not perfectly imaged by EOM, is still a lot better than on the Kirchhoff migrated section, where the crests are over-migrated, making identification of the different layers very difficult. The Heart Mt. Structure (A), Mt. Yamnuska (B) and the Lac des Arcs thrust are all better imaged on the EOM result.

Using iterative NMO-DMO-INMO (inverse NMO) - velocity analysis to obtain a velocity model for migration

Four iterations of NMO-DMO-INMO-velocity analysis on CDP gathers have been performed to build an RMS velocity model deterministically for use in prestack Kirchhoff time migration (Figure 12 b). This was done only over the central part of the model due to time constraints. Velocity analysis was done every 1 km. This is to be compared with the EOM result (Figure 12a), where velocity analysis was also done every 1 km. EOM imaged the small scale features of the Heart Mt. Structure (indicated by arrows) better, and provided an overall better resolution. The event indicated by "x" on Figure 12a can be made continuous by removing the 30% NMO stretch in the NMO correction module, as was done for Figure 12b. The EOM result can be greatly improved by doing more closely spaced velocity analysis as was shown in Figure 9b.

Figure 12c shows the resulting Kirchhoff poststack depth migrated section if the assumed RMS velocity model (used for Kirchhoff prestack time migration) had to be converted into interval velocities in depth as required for depth migration. The bad image (Figure 12c) shows that the four iterations described above did not correct for the high stacking velocities associated with the steep dips. Hence, conversion of the assumed RMS velocities into interval velocities in depth gave erroneous values for the interval velocities, which resulted in a bad depth image. A more elaborate method of building the velocity model in depth is required.

Time versus depth migration

Figure 13a and 13b compare Kirchhoff prestack depth with prestack time migration. The known velocity model was used in each case. The time migrated image deteriorates with increasing depth. Depth migration, however, correctly images the deepest structures including the Panther Culmination (C) and the Footwall Syncline (D). This indicates that depth migration is required to properly image the whole model. These results show that the limitations encountered with EOM are time migration problems, and depth migration is required to overcome them.

DISCUSSION

The final image obtained with EOM is considered an improvement over the Kirchhoff prestack time migration with the known velocity model. Fault planes are more interpretable and there is less scattered energy. The events are better focussed and show more structural detail, even in areas of strong lateral velocity variations and steep dips.

The final Equivalent Offset Migrated section improved with the following:

- Longer offsets in the creation of CSP gathers and velocity analysis. These provided better focussing of peaks on the semblance plots.
- Use of double-sided CSP gathers for velocity analysis, made identification of events easier and hence facilitated velocity picking on semblance plots.
- Addition of random noise to the synthetic data eliminated spurious peaks on the semblance plots and made velocity picking easier.
- Closer velocity analysis locations (every 100 or 500 m) especially in areas of steeper dips and small scale features (of 3 km or less) produced better final images
- Smoothing of the velocity model before stacking resulted in more continuous events and a better overall image.
- A velocity interpolator that follows the events will provide a more accurate velocity model with fewer analysis locations.
- Distortions to the diffraction shapes, as evident on CSP gathers (Figure 7a) shows why conventional prestack time migration results in poor imaging. These distortions indicate what possible steps may be taken to extend imaging capabilities of time migration.
- The migration velocities used for EOM tend to RMS velocities where good imaging occurs. The Panther Culmination was the only area that had the tilted diffraction curves, causing velocity errors. By using image rays, the velocity model built with EOM can be used to obtain an interval velocity model for depth migration.

The improved image obtained with EOM facilitates identification of the different horizons and structural geometries, hence enabling a better interpretation of the subsurface. The EOM result can thus be used to provide a more reliable interpretation to be used in velocity model building for depth migration, especially in areas where no velocity information is available.

FURTHER WORK

The next step is to interpret the EOM section and use it as a starting point for a depth velocity model. The time structure on the basement shows the time shape of the Kirchhoff diffraction curve. It will be useful to incorporate this time shift in the shape of the diffraction curve to eliminate the two "columns" of velocity values on the semblance plots (hence, eliminating the tilt problem of diffraction curves). In addition, the migration velocities may tend to RMS for the whole model, producing a more focussed time migrated image. RMS to interval velocity in depth conversion will then be possible, thereby obtaining a good starting velocity model for depth migration.

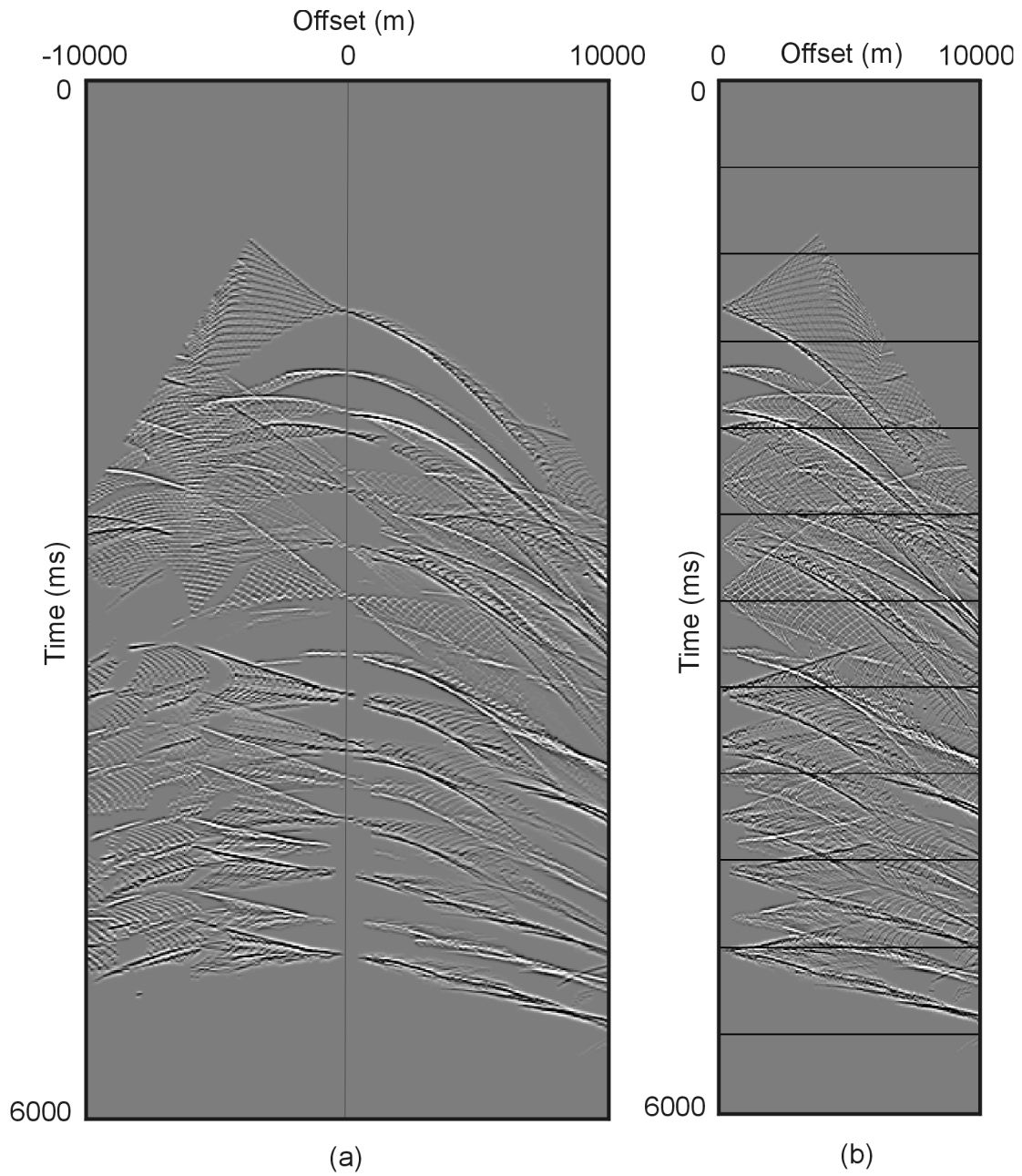
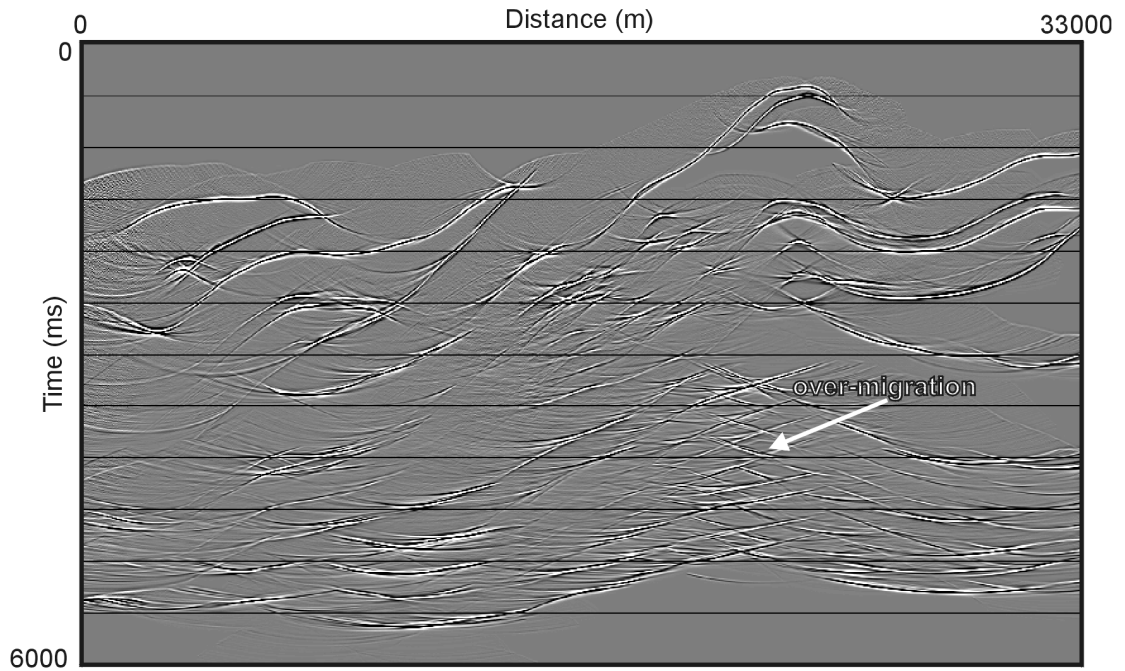
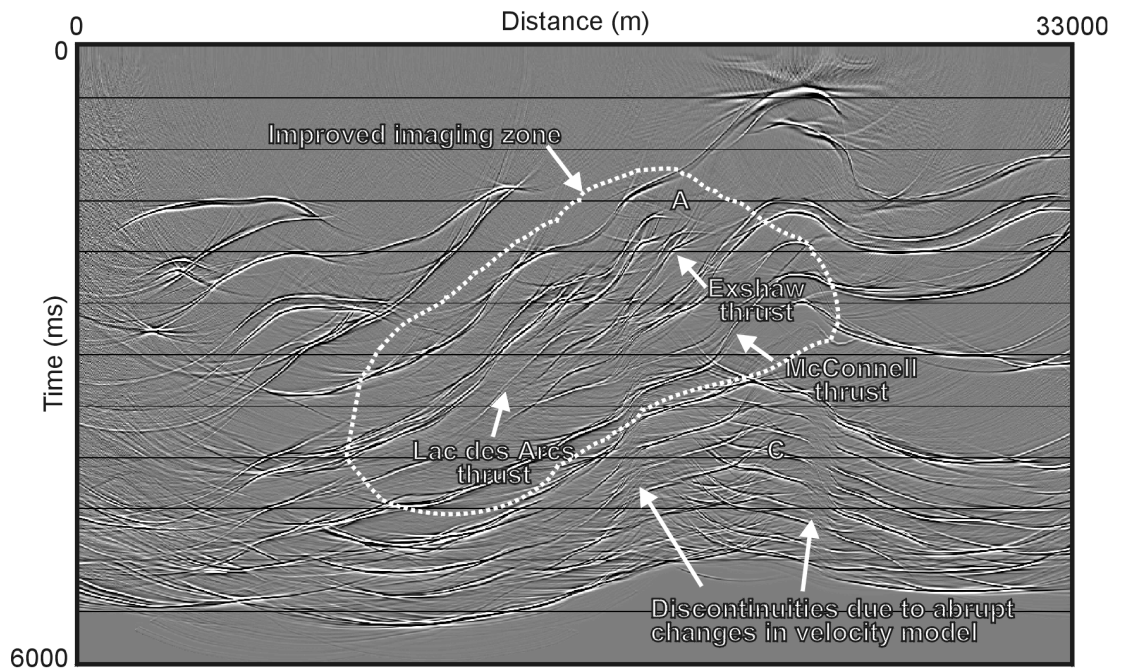


Fig. 8. A double-sided CSP gather (a) and a one-sided CSP gather (b) from the same location. Note how the double-sided gather makes identification of the different events easier.

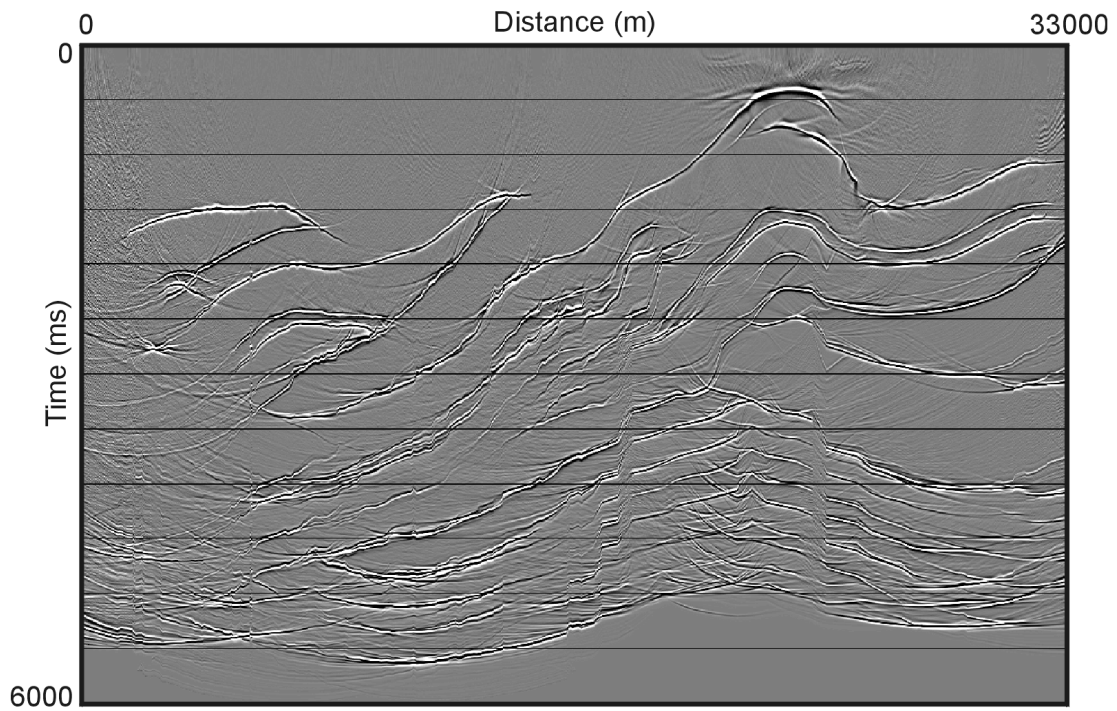


(a) velocity analysis every 3 km

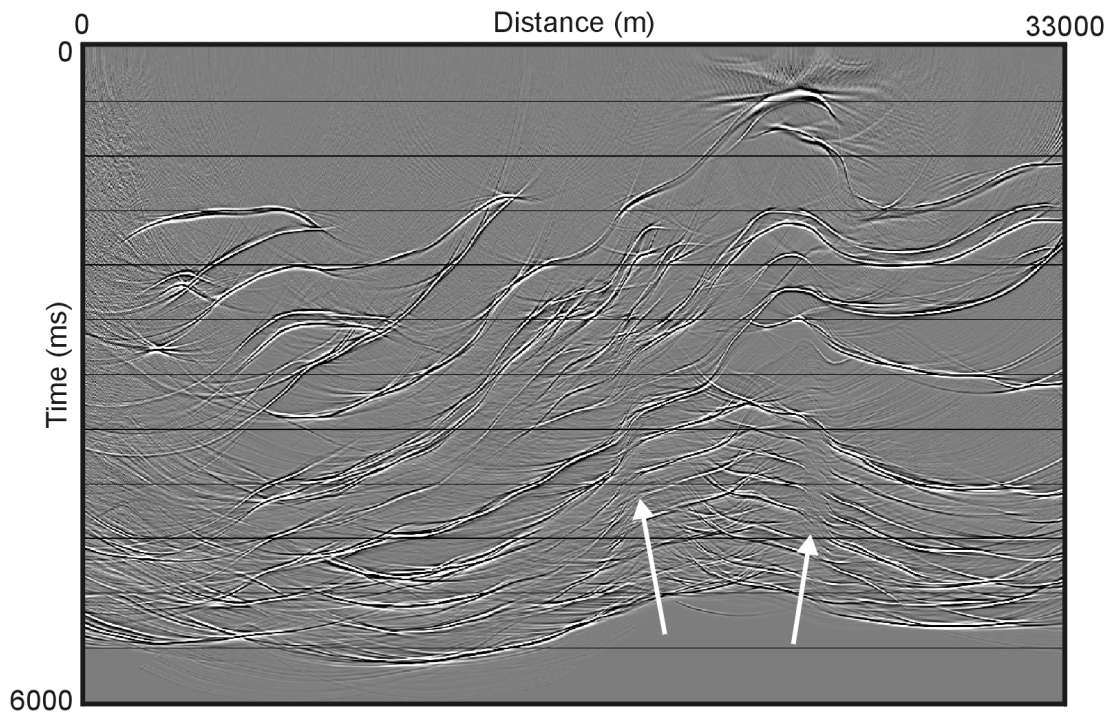


(b) Velocity analysis every 500 m

Fig. 9. Comparison of the effects velocity analysis location spacing can have on the final image: (a) velocity analysis every 3 km, (b) velocity analysis every 500 m. (b) gives a better overall image that is easier to interpret.

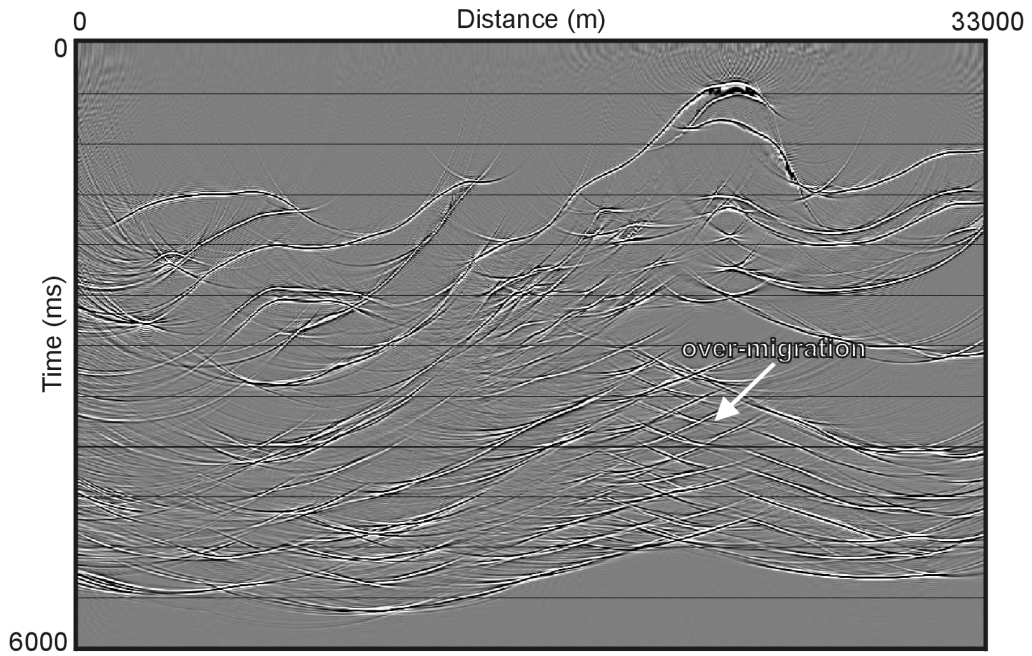


(a) EOM - velocity model not smoothed.

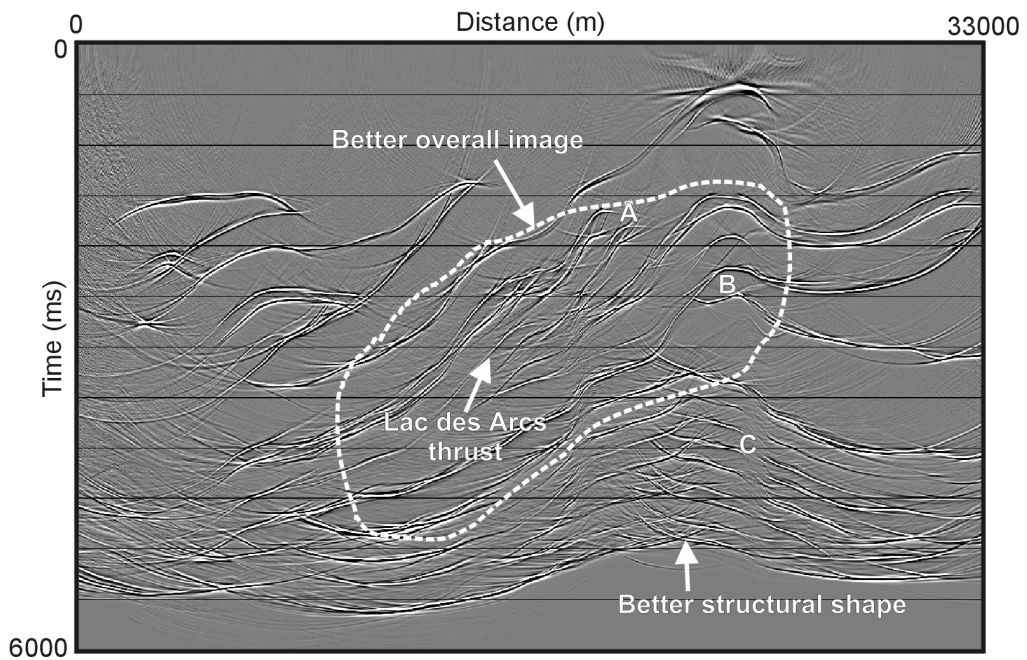


(b) EOM - smoothed velocity model.
Arrows indicate discontinuities due to abrupt velocity changes.

Fig. 10. Comparison of using an unsmoothed (a) and smoothed (b) velocity model for EOM. Events appear more continuous and better imaged when smoothing is applied (b).



(a) Kirchhoff pre-stack time migration with the known velocity model.



(b) Equivalent offset migration - velocity model derived from velocity analysis on CSP gathers.

Fig. 11. Comparison of Kirchhoff prestack migration with known velocity model and EOM.

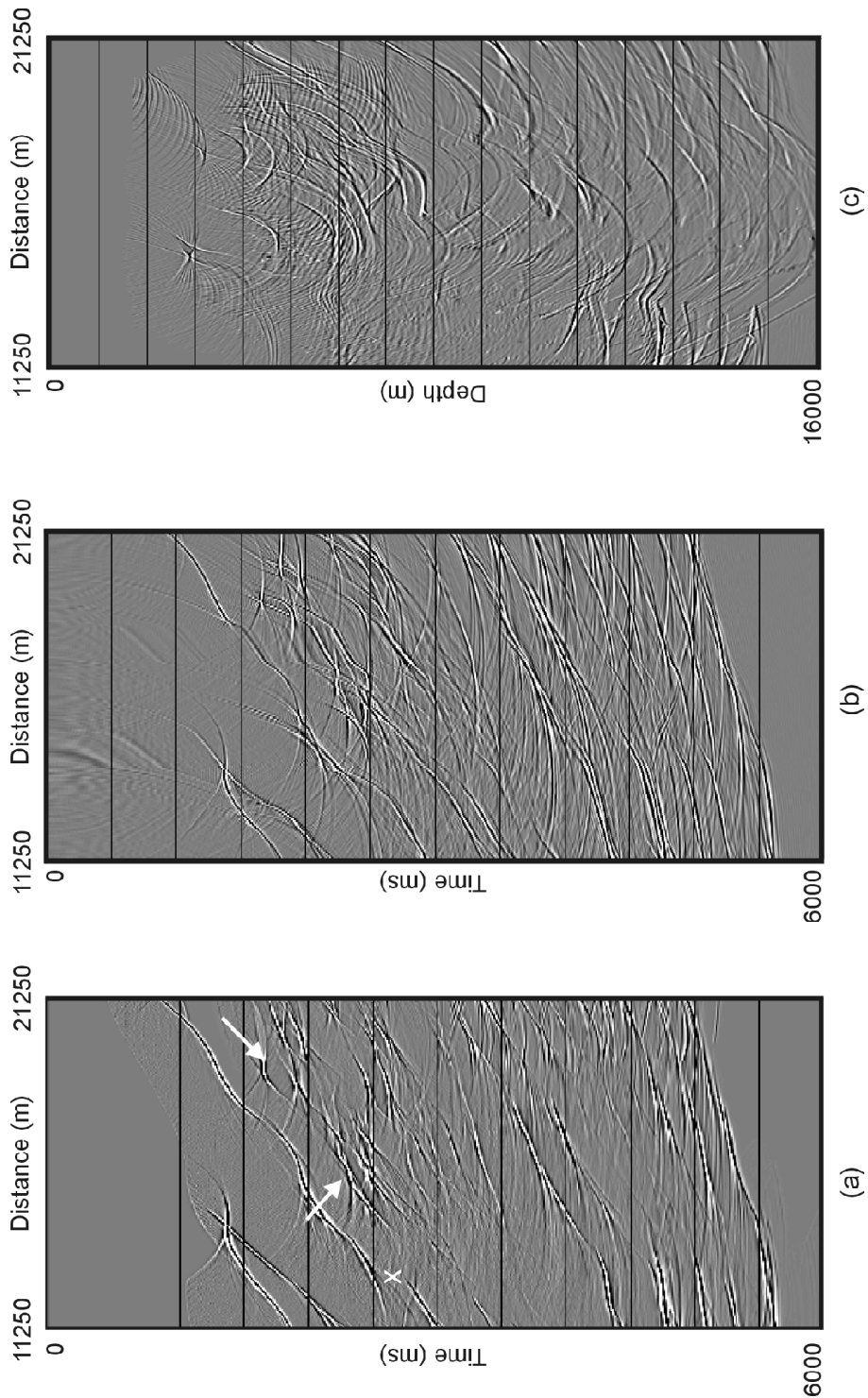
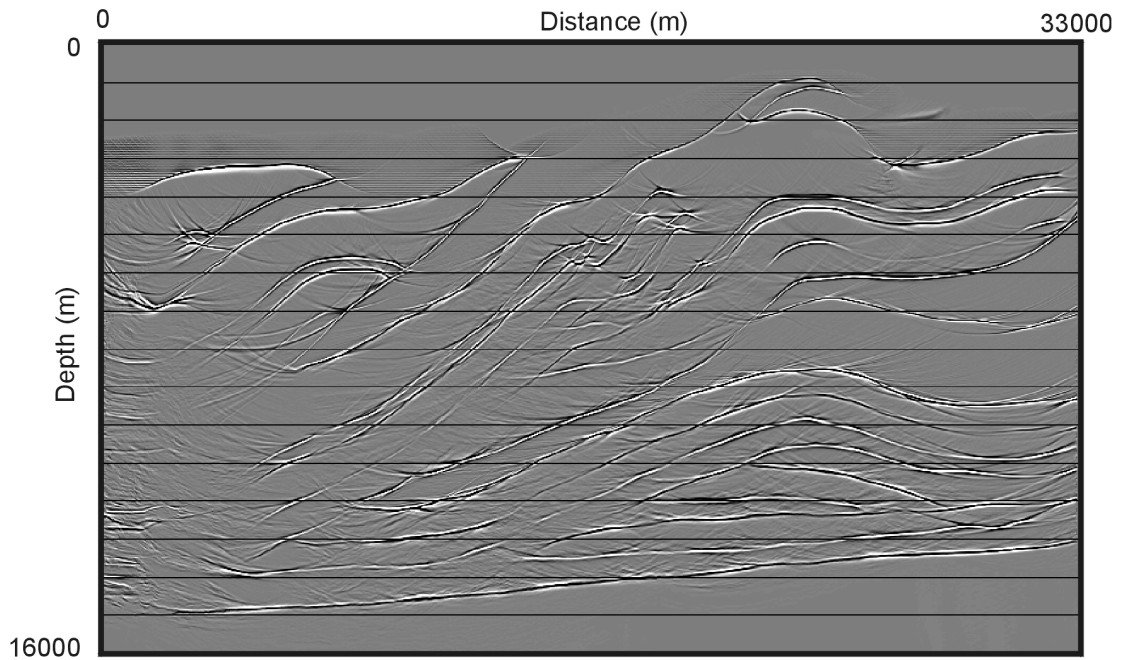
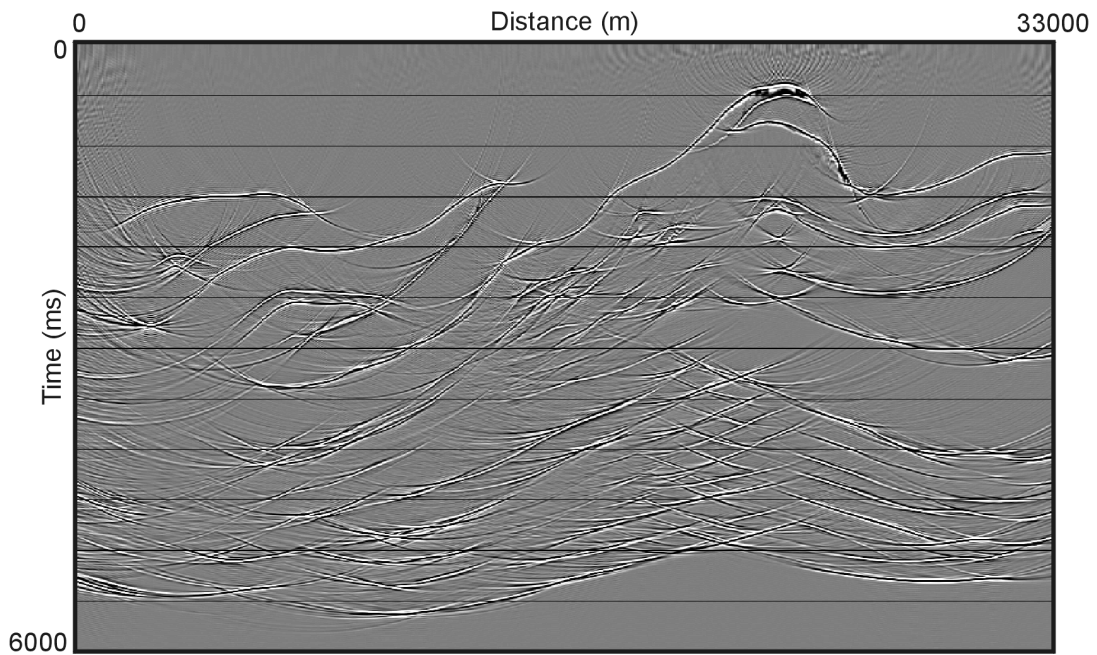


Fig. 12. Comparison of EOM with prestack time and poststack depth migration using a deterministic velocity model. (a) EOM with velocity analysis every 1 km (a much better image was obtained when velocity analysis was every 500 m - Figure 9b), (b) Kirchhoff prestack time migration and (c) Kirchhoff poststack depth migration. Velocity model for (b) obtained after 4 iterations of NMO-DMO-INMO-velocity analysis (every 1 km).



(a) Kirchhoff pre-stack depth migration with the known velocity model.



(b) Kirchhoff pre-stack time migration with the known velocity model.

Fig. 13. Comparison of Kirchhoff prestack depth and time migration with the known velocity model. The geometry of certain structures, like C and D, can only be well imaged with depth migration.

ACKNOWLEDGMENTS

We gratefully acknowledge the financial support for this work by Sponsors of CREWES and the Foothills Research Project, as well as the Natural Sciences and Engineering Research Council of Canada.

REFERENCES

- Bancroft, J.C., Geiger, H. and Margrave, G.F., 1998, The Equivalent Offset Method of Prestack Time Migration: in press for November - December 1998 issue of Geophysics.
- Kirtland Grech, M.G., Lawton, D.C. and Spratt, D.A., 1998, Numerical Seismic Modelling and Imaging of Exposed Structures: FRP Research Report, **4**, 1.1-1.36.
- Schultz, P. and Canales, L., 1997, Seismic Velocity Model Building: CE in Dallas, 2 November: The Leading Edge, **16**, No.7, 1063-1064.
- Taner, M. and Koehler, F., 1969, Velocity spectra - digital computer derivations and applications of velocity functions: Geophysics, **34**, 859-881.
- Yilmaz, O., 1987, Seismic Data Processing: SEG.